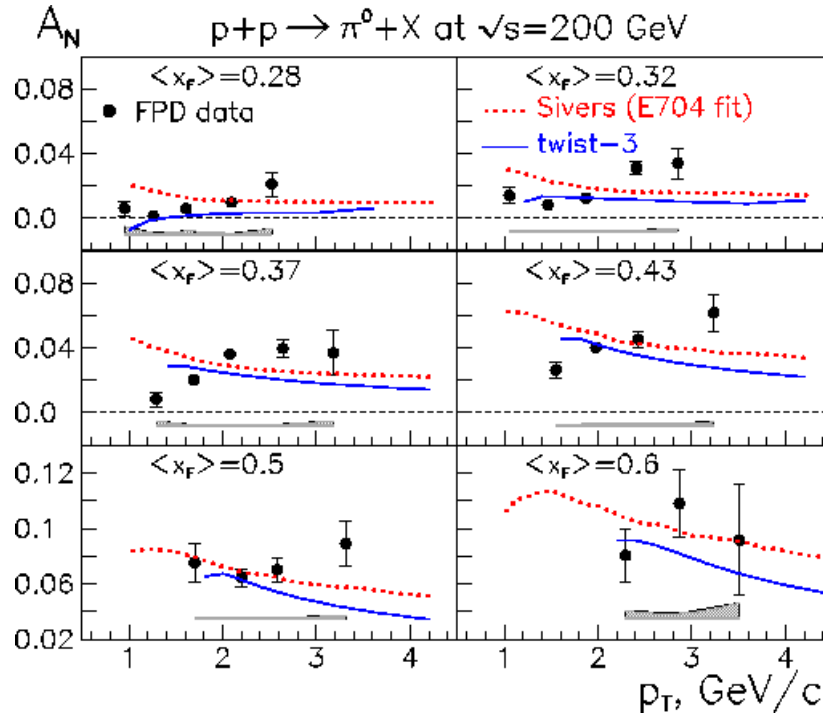


## Appendix E Transverse Spin

This appendix gives a more complete account of measurements completed at RHIC than in the Spin Plan update and a more complete account of plans for future measurements.

### E.1 Recent Transverse Spin Developments

As reported in the RHIC Spin plan update, the last successful RHIC spin run found very striking transverse single spin asymmetries for forward  $\pi^0$  production at  $\sqrt{s}=200$  GeV; forward  $\pi^\pm$  production at  $\sqrt{s}=62$  GeV; and forward  $\pi^0$  production at  $\sqrt{s}=62$  GeV. At the time of the update, only preliminary results from RHIC run 6 were available. Now, final results (Figs. 18, E-1,E-2) have been submitted by STAR [23] and BRAHMS [25] for publication.



**Fig. E-1** Transverse single spin asymmetries versus  $\pi^0$  transverse momentum ( $p_T$ ) in fixed  $x_F$  bins. Errors are as described for Fig. 18. The Sivers [65,66] and twist-3 [62] calculations are described in the Spin Plan update document.

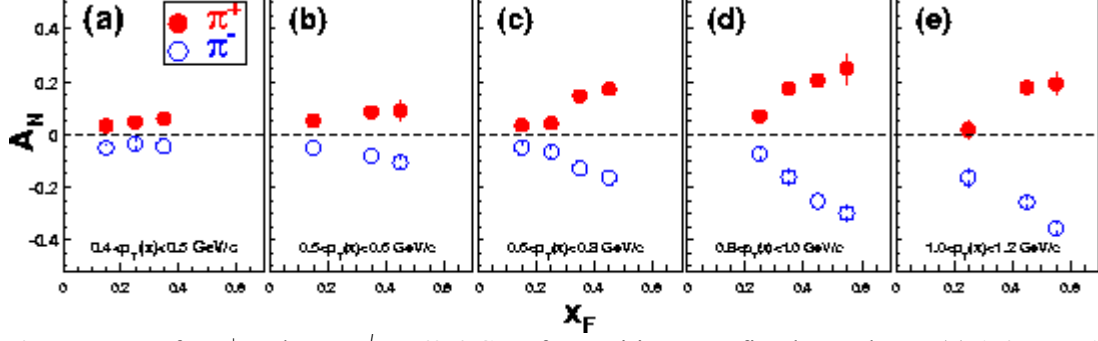


**Fig. E-2**  $A_N$  vs.  $x_F$  for  $\pi^+$  and  $\pi^-$  at  $\sqrt{s} = 62.4$  GeV for positive  $x_F$  at fixed  $p_T$  values: (a)  $0.4 < p_T < 0.5$ , (b)  $0.5 < p_T < 0.6$ , (c)  $0.6 < p_T < 0.8$ , (d)  $0.8 < p_T < 1.0$ , and (e)  $1.0 < p_T < 1.2$  GeV/ $c$ .

Even though the kinematics of the SIDIS measurement and the forward  $\pi^0, \pi^\pm$  data have little overlap, it is possible to account for most of the features of the RHIC data by calculations based on phenomenological fits to the SIDIS data. A key feature of the RHIC data that cannot be explained is the  $p_T$  dependence of the  $\pi^{0,\pm}$  single spin asymmetries at fixed  $x_F$ . Calculations based only on the Sivers mechanism require  $A_N$  to decrease with increasing  $p_T$ . This trend is not what is observed. New developments may suggest that this  $p_T$  dependence indicates the presence of Collins contributions to the single spin asymmetries.

In addition to results for  $p\uparrow+p \rightarrow \pi+X$ , the powerful Cerenkov-based particle identification capabilities of the BRAHMS forward spectrometer was exploited for measurements of transverse SSA for kaons and protons detected in the forward direction [25]. The observed  $A_N$  for  $K^+$  is consistent with expectations from u-quark dominance (Fig. E-3). Large asymmetries for  $K^-$  production contradict naïve expectations from valence quark scenarios. Measurements of  $A_N$  for protons detected in the forward direction (Fig. E-4) are consistent with zero, similar to observations made for  $p\uparrow+p$  at lower  $\sqrt{s}$ .

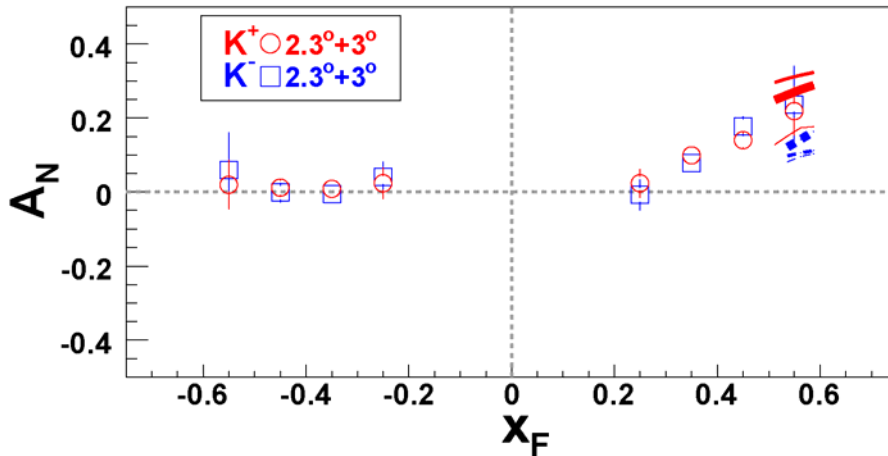


**Fig. E-3**  $A_N$  vs.  $x_F$  for  $K^+$  and  $K^-$  at  $\sqrt{s} = 62.4$  GeV for positive and negative  $x_F$ . Circle symbols are for  $K^+$  and box symbols are for  $K^-$  measured by combining data at  $2.3^\circ$  and  $3^\circ$  spectrometer settings. The solid ( $K^+$ ) and dotted ( $K^-$ ) lines are from the initial-state twist-3 calculations with (thick lines) and without (medium lines) sea- and anti-quark contribution [62]. Calculations for the Sivers function are shown as thin lines [66]. Errors are statistical only.

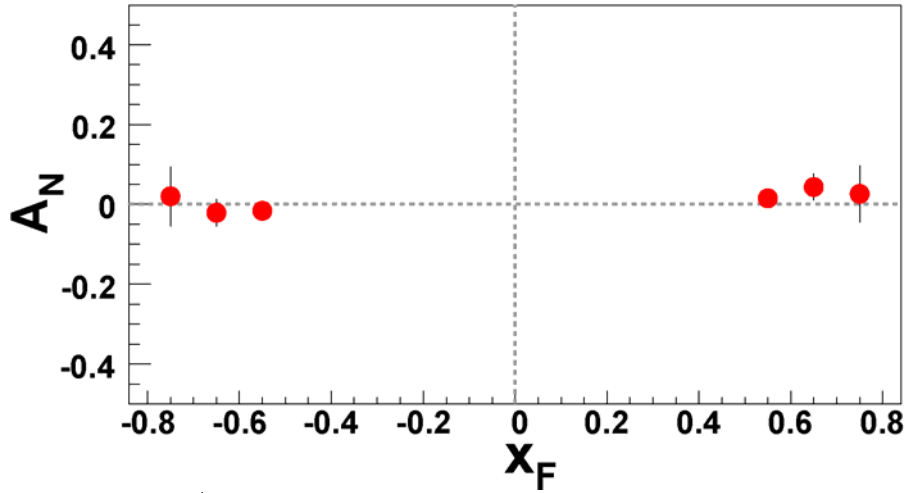


**Fig. E-4**  $A_N$  vs.  $x_F$  for at  $\sqrt{s} = 62.4$  GeV for protons detected at positive and negative  $x_F$ . Only statistical errors are shown where larger than symbols.

In addition to these final results submitted for publication, PHENIX has reported observations of analyzing powers that increase with  $x_F$  for  $x_F > 0$ , and null results for  $x_F < 0$ , from  $p\uparrow+p$  collisions at  $\sqrt{s}=62$  GeV for neutral pions reconstructed with their muon piston calorimeter [E1]. Also, BRAHMS has reported results for the  $x_F$  dependence of  $\pi^\pm$  production for  $p\uparrow+p$  collisions at  $\sqrt{s}=200$  GeV, albeit restricted to  $|x_F| < 0.3$  at this higher collision energy [E2].

Concurrently with the forward measurements, measurements of transverse spin asymmetries for midrapidity dijet production [36] were performed during RHIC run 6. The principle motivation was to directly measure the momentum imbalance between the jet pair ( $k_T$ ), and establish if it was correlated with the transverse polarization of the colliding protons as expected by the Sivers mechanism. This was initially proposed [68] as a means of constraining the gluon Sivers function. The kinematic coverage of the data is sufficient to begin to probe quark Sivers functions, extracted from the SIDIS measurements.

The null measurement for dijet spin asymmetries has led to a much deeper understanding of the Sivers mechanism. Although it is a necessary condition to have a spin- and  $k_T$ -dependent Sivers function, a TMD distribution function alone is not sufficient. There must also be a phase so that the required amplitude interference can give rise to the transverse single spin asymmetry. For SIDIS, this phase has a simple intuitive explanation [30]. The quark that absorbs the virtual photon does not propagate in free space following the interaction. Instead, it propagates in the chromomagnetic field generated by the spectator quarks. Since the proton is initially color neutral, this final-state interaction is necessarily attractive.

Once this phase was understood, it then became clear that the Sivers mechanism manifests itself in different ways in different hard scattering processes. The Drell Yan (DY) production of dilepton pairs has a particularly simple color structure, so can easily be understood. The final-state attractive color charge interactions in SIDIS become initial-state repulsive color charge interactions for the DY process, meaning that the Sivers functions between the two functions differ exactly by a minus sign [31].

The color structure for all of the quark and gluon scattering diagrams that enter in dijet production is much more complex than for DY production. Consequently, both initial-state and final-state interactions can occur. Their contributions can, and do, cancel.

This deeper understanding of the two requirements of the Sivers mechanism has led to a firm theoretical prediction. The transverse single spin asymmetry for  $\gamma$ +jet final states at RHIC energies will predominantly have initial-state color interactions [34], and hence are expected to be non-zero and opposite in sign from the Sivers functions extracted from SIDIS data. As discussed below, the experimental requirements for a  $\gamma$ +jet transverse spin measurement are substantially easier to meet than for a transverse spin DY measurement. Furthermore, the latter will require development of the luminosity and polarization for polarized proton collisions, and will require detector upgrades to STAR and PHENIX to enable a clean identification of the DY process.

## **E.2 Future Opportunities for Transverse Spin Measurements at RHIC**

The goals of future transverse spin measurements at RHIC can be stated as follows.

- In the long term, a transverse spin measurement of DY production is an essential test of the present theoretical understanding. In particular, if the predicted sign change is observed by experiment, then the presence of parton orbital motion within the spinning proton will be confirmed as a universal feature, and the fundamental expectation that unlike color charges attract and like color charges repel will be demonstrated. The requirements for a transverse spin DY experiment are understood, and make this an opportunity that could be realized in the latter years of this spin plan.
- In the immediate future, a test of the predictive power of the theory can be performed. In particular, experiments that would measure transverse SSA for  $\gamma$ +jet final states can establish the presence of initial-state color charge interactions. The present luminosity of RHIC and the capabilities of the experiments are sufficient to embark on this measurement.
- Also in the immediate future, separation of Collins and Sivers contributions can be realized. Also, interference fragmentation functions can be used to access the transversity distribution function.

### **E.2.1 Transverse-Spin and Drell Yan Production**

A document has been prepared [69] detailing what can be learned and what the requirements are for a measurement of transverse spin asymmetries for DY production of dileptons at RHIC. Consideration was given to the optimal collision energy. Based on the expected importance of valence quarks and the layout of the interaction regions, large rapidity dilepton pairs produced in collisions at  $\sqrt{s}=200$  GeV appears to be the optimal choice for a future experiment at PHENIX

and at STAR. PHENIX would detect  $\mu^+\mu^-$  with their muon arms. STAR could detect  $e^+e^-$  pairs at larger rapidity with its new forward meson spectrometer, but will require forward tracking capabilities to discriminate like-charge and unlike-charge pairs to fully assess the background. Expected sensitivity to the predicted transverse SSA based on Sivers functions extracted from the HERMES data is shown in Fig. 19, extracted from the more detailed writeup [69].

An important step to establish the feasibility of DY is to benchmark simulations against the dilepton decay of  $J/\psi$ . PHENIX has performed these studies, and requires isolation of the individual muons of the pair to reduce open heavy flavor backgrounds. The completion of the planned forward vertex detector and/or the nosecone calorimeter at PHENIX can provide the necessary isolation.

Following luminosity developments planned for RHIC-II and detector upgrades, it is expected that a transverse spin DY measurement could be completed in two 10-week runs in 2015 and 2016.

### **E.2.2 Transverse-Spin $\gamma$ +jet**

In the meantime, further theoretical work has proceeded. Specifically, there is a prediction that repulsive color charge interactions will produce a change in sign for forward  $\gamma$  + away-side jet in polarized proton collisions at  $\sqrt{s}=200$  GeV [20]. There are two implications of this prediction:

- (1) there is partonic orbital motion within the spinning proton, observable in a process dependent way in both SIDIS and polarized proton collisions;
- (2) the sign difference between SIDIS and polarized proton collisions demonstrates the reality of attractive and repulsive color charge interactions.

The addition of the forward meson spectrometer (FMS) prior to the start of run 8, and the away-side jet detection capabilities in the central region at STAR, uniquely positions the STAR collaboration to complete this measurement. It should be mentioned that the simple explanations, based on abelian (QED) analogies, of why there is a sign change in forward photon + away-side jet is not as intuitive as for transverse SSA for the DY process. Observation of the predicted sign change would bolster the case for a future transverse spin DY measurement at RHIC.

The STAR FMS (Fig. E-5) would be used for detecting direct photons at large rapidity. This device was built for studies of possible gluon saturation phenomena at RHIC. Run-8 results will address this question. The FMS is a hermetic electromagnetic calorimeter, built from finely segmented lead-glass detectors, positioned west of the interaction point at STAR. It views particles produced in collisions through large holes in the poletips of the STAR magnet. The integrated number of radiation lengths between the calorimeter and the interaction point is dominated by crossing the beryllium beam pipe.

The FMS is an outgrowth of the forward pion detector (FPD), corresponding to modular electromagnetic calorimeters built from finely segmented lead-glass detectors. Consequently, extensive experience with event reconstruction for both simulation and data exists from the FPD project, and can be carried over to the FMS. In general, full PYTHIA/GEANT simulations

accurately account for what has been observed in the FPD. Single beam backgrounds are minimal, as confirmed in Run 8 by long dwell time vernier scans, due to shielding provided by the cryostats of the RHIC magnets. Comparison between simulation and data for the FMS awaits final calibrations.

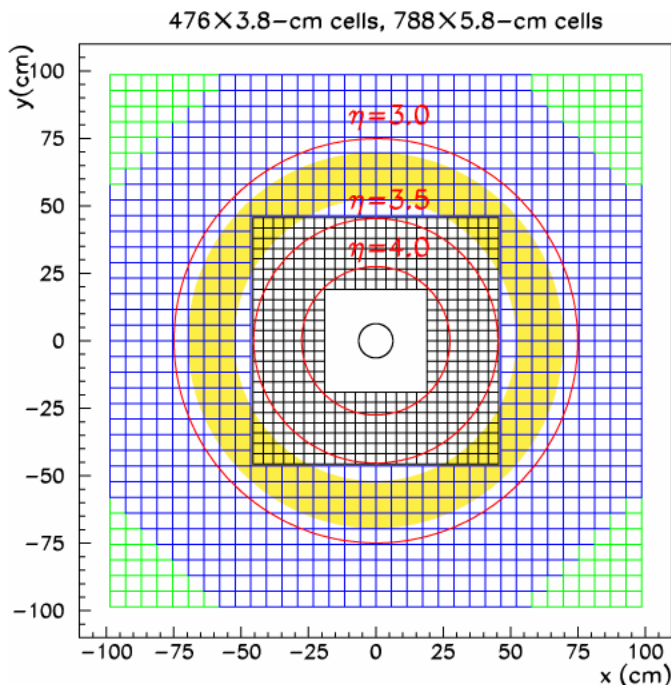


**Fig. E-5** A schematic of the STAR forward meson spectrometer as seen from the interaction point. The Blue beam penetrates into the page at the center of the matrices. The yellow shaded area represents a conservative fiducial volume used for detection of direct  $\gamma$  candidates, with the remainder of the FMS used as a veto of photons arising primarily from  $\pi^0, \eta$  decay.

For direct photon detection with a large-area hermetic electromagnetic calorimeter, the most effective method is to eliminate other sources of photons by direct detection. These other photon sources arise primarily from the decay of  $\pi^0$  and  $\eta$  neutral mesons. Multiple aspects make this feasible with the FMS. First, because the calorimeter is at large rapidity, the typical photon energies are large ( $E_\gamma > 35$  GeV) and the hadronic response of the FMS is small. Direct simulation of the detector response via GEANT simulations employing the GEISHA hadronic simulation, applied to full PYTHIA events of collisions, have demonstrated that the hadronic response of the lead glass detectors is minimal for energy depositions in excess of 25 GeV. Second, the large Lorentz factors result in significant spatial correlations for the decay products from  $\pi^0$  and  $\eta$  mesons. For example, when there is a candidate direct photon having  $E_\gamma = 25$  GeV, 95% of the phase space for all  $\pi^0$  decays that could potentially be the source of this energetic photon are contained in a circle of radius 23 cm (approximately four large cells of the FMS) around the 25-GeV photon at the face of the FMS. Finally,  $\pi^0$  and  $\eta$  mesons are most typically produced via fragmentation in p+p collisions at RHIC energies. This means that other hadrons share the energy of the fragmenting quark or gluon, softening the decay photon spectrum. The daughter photons from  $\pi^0$  and  $\eta$  decay then further divide this energy. In contrast, direct photons are produced in the hard scattering process. Their energy is not shared via fragmentation nor is it

shared by particle decay. The energy where direct photon probabilities exceed decay photon probabilities is  $\sim 50$  GeV for  $\langle \eta \rangle \sim 3.2$ , with no other conditions on the event. The  $\pi^0$  and  $\eta$  backgrounds can be reduced, and this energy can be lowered to  $\sim 25$  GeV, by subdivision of the FMS into two volumes. The fiducial volume, used for identifying direct photon candidates, is a small annular region within the outer calorimeter. The remainder of the FMS is used as a veto to establish that other photons from the decay of neutral mesons are not present. The effectiveness of the discrimination between direct and decay photons is demonstrated via full collision event simulations in Fig. 7.

Restricting the measurement of the forward photon to  $E_\gamma > 35$  GeV at  $\langle \eta_\gamma \rangle = 3.2$  produces a signal:background ratio of 2.1. Lower thresholds result in larger contamination, and so are undesirable. Substantial gains in yield can be realized by small changes in the fiducial volume towards smaller distance from the beam because of the very strong power law dependence on  $p_{T,\gamma}$ . A detailed optimization of signal magnitude and signal:background ratio still must be completed.

Fragmentation photons are also a background for inclusive direct photon measurements that would require a careful study of jet asymmetries for forward jets that contain a fragmentation photon. The prediction for the sign change for transverse SSA is for a forward photon + recoil jet. The isolated forward fragmentation photon will have its momentum balanced by two jets, rather than one, as expected for direct photons by the dominant  $qg$  Compton diagram. Consequently, the fragmentation photon contribution will be spread throughout a  $\Delta\phi = \phi_{\text{jet}} - \phi_\gamma - \pi$  distribution, whereas the signal of interest is on the sides of the peak in the  $\Delta\phi$  distribution, in the vicinity  $\Delta\phi \approx 0$ . More detailed simulations to quantify this argument are in progress.

An estimate of the luminosity necessary for this measurement has been made based on simulations of the  $\Delta\phi$  distribution for  $p+p \rightarrow \gamma(\text{forward})+\text{jet}$  at  $\sqrt{s}=200$  GeV (Fig. 19). The simulations use a simple clustering algorithm to define the midrapidity jet, requiring a seed with transverse energy of at least 0.5 GeV. A cone radius,  $R = (\delta\phi^2 + \delta\eta^2)^{1/2} = 0.7$  is used in the clustering. Here,  $\delta\phi(\delta\eta)$  refer to the deviation of a hadron from the thrust axis of the reconstructed jet. Jet reconstruction, even at  $p_{T,\text{jet}} > 2$  GeV/c, is found robust by comparison to recoil parton kinematics and by comparison to a leading particle analysis. The result is that  $10^4$  useable forward photon + jet coincidences are expected in a  $30 \text{ pb}^{-1}$  data sample with 65% beam polarization. The  $\gamma(\text{forward})+\text{jet}$  yield is sensitive to the jet-finding parameters and the fiducial volume requirement for the forward photon. A full optimization of the event selection to test the theoretical prediction is required, and possibly could result in robust sensitivity to the predicted sign change ( $>4\sigma$ ) at smaller figure of merit. An initial sample of transverse spin  $\gamma(\text{forward})+\text{jet}$  of  $6 \text{ pb}^{-1}$  recorded with beam polarization of 60% would be used to fine tune the figure of merit requirements for the measurement. This data sample would correspond to an order of magnitude increase beyond what was acquired including all tracking detectors of STAR during RHIC run 8.

### E.2.3 Future Transversity Studies at RHIC

Since the measurements of the transverse spin distribution function is always combined by yet another chiral-odd object it is fairly difficult to access it. At RHIC the figure of merit for Drell Yan double spin asymmetries  $A_{TT}$  is not favorable in the light of the very small predicted asymmetries [E3]. These small asymmetries are dominated by the expected small sea quark transverse polarizations and the increasing denominator from the unpolarized cross section.

Instead of combining the chiral-odd transversity distribution with another chiral-odd transversity distribution it can also be combined with chiral-odd fragmentation functions. The most prominent of them is the Collins function which describes the fragmentation of a quark with transverse spin by the azimuthal distribution of a detected hadron around the quarks momentum axis. While the quark direction is directly known at leading order in semi-inclusive DIS it has to be approximated by the jet direction in pp collisions. Therefore it can best be measured the central detector of STAR where one can reconstruct jets fairly well. However, as transversity is expected to be mostly a valence quark effect the asymmetries in the central region might not be too large. In the forward regions one is more sensitive to higher  $x$  and thus expects larger asymmetries. The capability of reconstructing jets and in particular charged hadrons is quite limited in the forward regions, but one could use a high energetic  $\pi^0$  as a jet proxy and study the azimuthal distribution of another  $\pi^0$  around this axis. Using a high-energetic hadron instead of a reconstructed jet will smear the reconstructed angles and thus the azimuthal modulations, but it should still be possible to obtain a reasonable measurement using the FMS in STAR and the muon piston calorimeter in PHENIX.

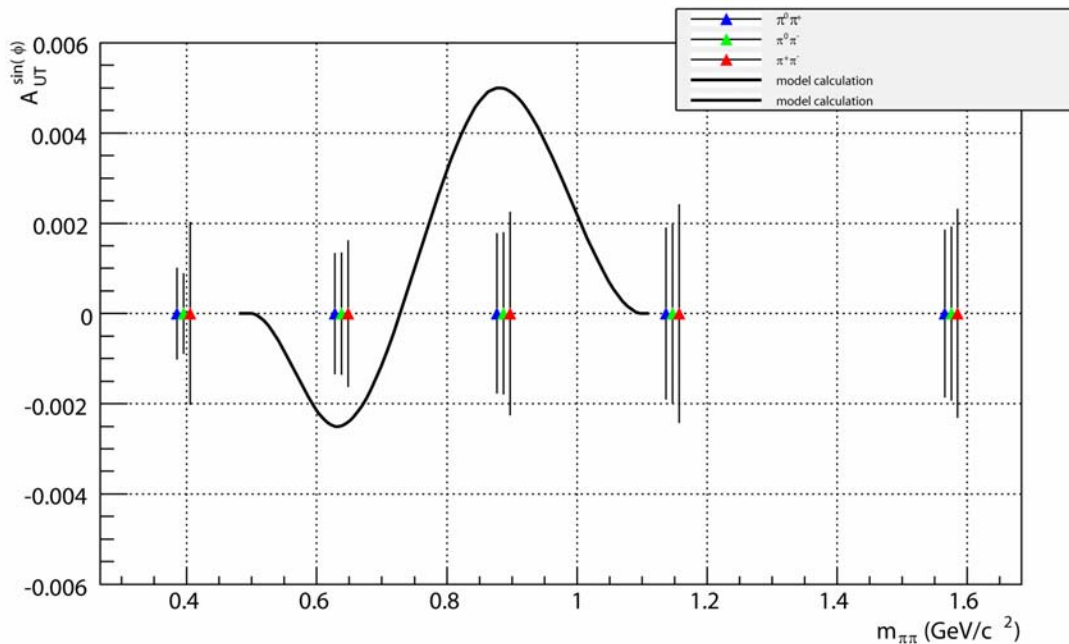


**Fig. E-6** Single spin asymmetries  $A_{UT}$  for  $\pi^+\pi^-$  (red) and  $\pi^+\pi^0$  (blue) and  $\pi^-\pi^0$  hadron pairs as a function of the invariant mass of the hadron pair. The data points correspond to the statistical errors expected with  $16 \text{ pb}^{-1}$  and 65% polarization in run 9. The continuous line corresponds to a prediction from for the interference fragmentation function and a transversity distribution as obtained in [40].

A second chiral-odd fragmentation function is the interference fragmentation function which describes the fragmentation process of a quark with transverse spin into a hadron pair where the final state hadrons interfere between s and p channels. This function also results in an azimuthal distribution of the plane spanned by the two hadrons along the momentum of the struck quark and its transverse spin. This type of asymmetry measurement has been described by [40] for pp and can be performed well in the central detectors of PHENIX and STAR for  $\pi^+\pi^-$ ,  $\pi^\pm\pi^0$  and similarly with kaons.

The expected asymmetries for the 2009 run, assuming  $16\text{ pb}^{-1}$  and 65% polarization in the  $\pi^+\pi^-$ ,  $\pi^\pm\pi^0$  channels in the central arms of PHENIX can be seen in Fig. E-6 assuming a transversity distribution as obtained from the SIDIS and Belle fit [40] and a sizeable interference fragmentation function based on a prediction from [42] as a function of the invariant mass.

### **Additional References**

[E1] M. Chiu (PHENIX), Proc. of the 17<sup>th</sup> International Spin Physics Symposium (SPIN2006) [arXiv:nucl-ex/0701031].

[E2] F. Videbaek (BRAHMS), Proc. of XIII International Workshop on Deep Inelastic Scattering (DIS07) [arXiv:nucl-ex/0508018]; F. Videbaek (BRAHMS); Proc. for PANIC 2005 [arXiv:nucl-ex/0601008].

[E3] H. Kawamura, J. Kodaira, K. Tanaka, [arXiv:hep-ph/0801.3087].